JAAS

Improved Uranium Isotopic Ratio Determinations for the Liquid Sampling-Atmospheric Pressure Glow Discharge Orbitrap Mass Spectrometer by use of Moving Average Processing

Journal:	*Journal of Analytical Atomic Spectrometry*
Manuscript ID	JA-ART-10-2021-000374.R1
Article Type:	Paper
Date Submitted by the Author:	04-Mar-2022
Complete List of Authors:	Goodwin, Joseph; Clemson University, Department of Chemistry Manard, Benjamin; Oak Ridge National Laboratory, Chemical Science Division Ticknor, Brian; Oak Ridge National Laboratory, Chemical Sciences Division Cable-Dunlap, Paula; Oak Ridge National Laboratory, Nuclear Nonproliferation Division Marcus, R.; Clemson University, Chemistry

Improved Uranium Isotopic Ratio Determinations for the Liquid Sampling-Atmospheric Pressure Glow Discharge Orbitrap Mass Spectrometer by use of Moving Average Processing

Joseph V. Goodwin[1], Benjamin T. Manard[2], Brian W. Ticknor[2], Paula Cable-Dunlap[3], and R. Kenneth Marcus[1*]

[1] - Department of Chemistry, Clemson University, Clemson SC 29634

[2] - Chemical Sciences Division, Oak Ridge National Laboratory, Oak Ridge, Tennessee 37830

[3] - Nuclear Nonproliferation Division, Oak Ridge National Laboratory, Oak Ridge, Tennessee 37830

* - Corresponding Author: marcusr@clemson.edu

Submitted for publication in the Journal of Analytical Atomic Spectrometry

Abstract

The liquid sampling-atmospheric pressure glow discharge (LS-APGD) is a versatile combined atomic and molecular (CAM) ionization source capable of ionizing elemental species, small polar compounds, low-polarity polycyclic aromatic hydrocarbons, and proteins. While the LS-APGD has been proven capable of determining the $^{235}U/^{238}U$ isotope ratio in enriched and natural uranium, recent efforts have strived to reduce the analysis time of individual measurements by employing higher-order data processing techniques, specifically, moving average methods. The use of a moving average (of data windows of various widths) improves the precision of the ratio measurements and reduces the number of scans needed to be collected to generate high-precision results. Additionally, use of the moving average minimizes the quantity of sample that needs to be analyzed while reducing the measurement time. These reductions have allowed isotope ratio (IR) determinations to be made using injections instead of direct infusion of the analyte. For example, employing a 40-point window width in the moving average to direct infusion data reduced the percent relative standard deviation (%RSD) of the $^{235}U/^{238}U$ values from 3.4% to 0.5%. For the injection of a 100 μL aliquot, the %RSD was reduced from 5.3% to 0.7%.

Introduction

Isotope ratio (IR) determinations have implications for a multitude of diverse scientific disciplines. In geochemistry, isotope ratio determinations of radioactive constituents allow for determination of the dates of specific geological events.[1] In forensic sciences, isotope ratios have been used for source identification in numerous applications, including analyzing explosives, ignitable liquids, illicit drugs, paints, soils, fibers, tapes, plastics, safety matches, microbial studies, documents, and poisons.[2, 3] Nuclear forensics uses isotope ratio measurements to generate signatures of known materials, which can be compared to measurements collected from seized nuclear materials, providing information on the material's origin and history.[4-6] Isotope ratio measurements are one of the many tools used by the nuclear safeguards community to verify declarations made by states regarding the status and nature of their nuclear program; thus, the practical aspects of the determination of U^{235}/U^{238} isotope ratios are of continuing interest.[7, 8]

Traditionally, high precision isotope ratio measurements of uranium and other actinides are performed using thermal ionization mass spectrometry (TIMS) or multi-collector inductively coupled plasma mass spectrometry (MC-ICP-MS).[9-13] While the current benchmark methods, TIMS and MC-ICP-MS, are not without drawbacks. TIMS instruments are large, complex, expensive, and often require extensive and complicated sample preparation techniques prior to analysis.[11] MC-ICP-MS instruments are also costly with large footprints, but the methods do not require as extensive sample preparation as typically required for TIMS. However, chemical separations are often required to remove molecular and elemental isobaric interferences before analysis.[14, 15]

In addition, MC-ICP-MS instruments require plasma gas flow rates of up to 16 L min^{-1},[16] contributing to the operational overhead. While both platforms provide excellent performance, it would be advantageous to have the capacity to deliver performance for the intended purpose on less complex, lower cost, and higher throughput instruments. Taken a step further, instruments that are operable in less sophisticated environments, perhaps field deployable, would also be desirable.

In an effort to reduce the complexity, the footprint, and capital costs of isotope ratio determinations, a microplasma ionization source, the liquid sampling-atmospheric pressure glow discharge (LS-APGD), has been coupled to a benchtop Thermo Scientific Q Exactive Focus Orbitrap FTMS.[16-20] The LS-APGD ionization source, developed by Marcus and co-workers, operates at low power consumption (<50 W) and low solution flow rate (<100 µL min^{-1}), with total consumption of analyte solutions.[21] In addition to elemental analysis, the LS-APGD functions as a combined atomic and molecular source, capable of ionizing small polar molecules, low-polarity polycyclic aromatic hydrocarbons, and proteins.[22-28] The LS-APGD's ability to successfully couple to instrumentation typically reserved for molecular mass spectrometry while having minimal gas, solution, and power requirements has allowed advances to be made towards simplified instrumentation, lower cost, and higher mass resolution performance in isotopic ratio analysis. Indeed, the ultra-high resolution afforded by the orbitrap analyzer has the potential to greatly lower the need for complex sample clean-up, as demonstrated in the ability to mass resolve ^{87}Sr and ^{87}Rb ($m/\Delta m > 350$ k).[26] With regards to uranium isotopic ratio measurements, a first-level comparison of the measurement precision between the microplasma/Orbitrap combination, TIMS,

scanning sector-field, and quadrupole ICP-MS across a range of degrees of isotopic depletion/enrichment displayed comparable levels of performance between the microplasma approach and the more widely applied methods.[20] This was particularly true for the samples of ^{235}U enrichment, a reflection of the limited dynamic range of the standard Orbitrap data system. That study provided the impetus for the continued development of the present methodology with regards to yielding a practical approach to high precision uranium isotope ratio analysis. It is yet a further goal of subsequent efforts to address methods of performing higher accuracy measurements.

Previous efforts regarding uranium isotope ratio measurements with the LS-APGD/Orbitrap coupling looked at many different aspects of plasma operation, use of collisional dissociation, the roles of concomitant ions, and advanced data acquisition systems.[16, 20, 24, 26, 29] The measurement of the natural abundance $^{235}U/^{238}U$ ratio of ~0.0072 represents a non-trivial challenge in terms of the dynamic range and stability of an analytical system. The present effort focuses on a means of reducing the analysis time required to reach targeted levels of isotope ratio precision. The typical spectral acquisition workflow has consisted of 100 scans, each consisting of 10 microscans. One microscan entails the injection of an ion packet from the C-trap (where ions are initially accumulated), with a subsequent 100 millisecond signal (transient) acquisition, with the individual time-domain transients averaged prior to processing.[20] Transients (signals vs. time) are Fourier transformed using an enhanced Fourier transformation technique (eFT) to yield frequency domain spectra which are directly correlated with ion m/z[16, 30] using the manufacturer's standard data acquisition hardware and computational methods. Additional details on the eFT technique used with orbitrap mass

spectrometers have been described.[30] A complete isotope ratio analysis to this point has consisted of the average of 3, 100-scan acquisitions, with each sample analyzed in triplicate.[20] The work presented in this manuscript investigates the potential to reduce the 100-scan acquisition protocol by using an alternative data processing method, specifically a moving average. While moving averaging has been used previously with ion cyclotron resonance (ICR) FTMS instruments,[31] to the authors' knowledge, this is the first instance reported of using a moving average approach to improve the precision of isotope ratio determinations, regardless of the spectrometer platform. The approach is suggested to be effective in reducing the number of scans (i.e., analysis time) to achieve the precision for a specific application, both in the case of continuous sample solution infusion as well as the analysis of volume-limited samples via discrete injections. It is believed that the approach holds promise for other quantitative measurements on FTMS (ICR and Orbitrap) instruments as well.

It should be noted that accuracy is not discussed in this manuscript as accuracy cannot be effectively explored until the targeted analytical precision has been optimized. Future studies will focus on accuracy with the application of mass bias corrections as is common for many forms of isotope ratio determinations.[32, 33]

Experimental

A dual-electrode LS-APGD ionization source, as previously described[24] and depicted in Fig. 1, was operated at a solution flow rate of 30 μL min^{-1}, with a discharge current of 30 mA per electrode, an electrode gap distance of 1.5 mm, and a helium flow rate of 0.5 L min^{-1} for all analyses. The LS-APGD source consists of two stainless steel anode electrodes (weldable feedthrough, MDC Vacuum Products, LLC, Hayward,

California.) The solution cathode consists of an outer stainless-steel capillary (0.04 in I.D., 1/16 in O.D.; McMaster Carr, Elmhurst, IL) that delivers the helium sheath gas with a fused silica inner capillary (250 μm I.D., 360 μm O.D.; Molex, Lisle, IL) that delivers the analyte solution to the plasma. The plasma is generated between the solution cathode and the anodes. Power, solution flow, and gas flow are controlled through a custom control box (GAA Custom Electronics LLS, Kennewick, WA). The 2% nitric acid carrier electrolyte solution was prepared by diluting 70% Nitric acid (BDH/VWR, Radnor, PA) with deionized water prepared from an Elga PURELAB flew water purification system (18.2 MΩ cm^{-1}) (Veolia Water Technologies, High Wycombe, England). A natural-abundance uranium standard (3 g L^{-1}) (High Purity Standards, Charleston SC) was diluted to 100 ppb in 2% nitric acid. A $^{235}U/^{238}U$ value of 0.007277 was determined by MC-ICP-MS by the ORNL collaborators.

A Thermo Scientific Q Exactive Focus Orbitrap mass spectrometer was used with no modifications other than removing the ESI source. A six-port two-position Rheodyne 7125 injection valve with a 100 μL injection loop was used for discrete sample analysis. Akin to other plasma-based ionization sources, instrument 'warm-up' was accomplished by operation of the plasma solely on the electrolyte solution for typically 30-60 min. Direct infusion measurements were made after 5 min of initiation of the sample flow, with each acquisition consisting of 100 scans, with each scan made of 10 microscans. A complete sample analysis consists of 3 acquisitions. Using this protocol, each acquisition takes approximately 5 min, using 0.14 mL of test solution. Data acquisition was begun approximately 60 min following the initiation of flow to allow for plasma stabilization. Discrete sample injections were made into the plasma

operating with electrolyte solution flow, including 154 scans, each scan made of 10 micro scans. The number of scans collected during injection analysis represents initiation at the moment of injection to account for the dead volume between the injector and LS-APGD. Typically, injection measurements are made using just the transient maximum for determinations; however, for the application of moving average analysis, points from the transients' front and trailing edges were included to use the full sample response. By utilizing the transient front/tails, the number of scans included was increased to approximately 100 in comparison to the approximately 50 scans covering just the transient plateau.

All measurements were made in the positive ion mode. The ion transfer capillary temperature was set to 250°C, the quadrupole bandpass range was set to 268.5 ± 25 Da, and the signal digitization range was set to frequencies corresponding to 268.5 ± 5 Da. The injection time of 100 ms with automatic gain control (AGC) target of 1 million charges was used. The resolution was set to m/Δm of 70,000 (m/z = 200). A higher-energy collisional dissociation (HCD) energy of 120 eV and an in-source collision dissociation energy of 90 eV was used to remove clusters related to water and nitric acid.[34] Measurements were made using uranium dioxide cation (UO_2^+) species, per previous efforts.[20]

Moving Average Methodology - Moving average, commonly referred to as a simple moving average, is a powerful time-domain filtering process that is frequently used to minimize the impact of random noise on the data collected.[35, 36] A moving average consists of selecting a window (sometimes referred to as a boxcar) size in terms of the number of data points and averaging all points within that boxcar. Other similar forms of

data processing have been reported, with Savitzky-Golay smoothing being a prominent example. Savitzky-Golay smoothing uses a set of weighted coefficients and a normalization constant to replicate least-square fitting of a polynomial, typically a quadratic or quartic, through a set of data points.[37-39] Moving average analysis can be viewed in terms of Savitzky-Golay smoothing as fitting the data to a zero-degree polynomial (a non-zero constant flat line) where the coefficients are all one (unweighted), and the normalization factor is equal to the number of data points in the boxcar.[39]

For this application, a data point is one scan (consisting of 10 micro scans)/mass spectrum and the individual isotopic signals therein. This process is graphically represented in Fig. 2 for a typical 100 µL injection total ion current chromatogram. In this example, a 10-point would contain points 35-44. The boxcar is then moved along the x-axis by one point (adding the new point to the end of the window while dropping a point at the origin), and the points within the window are averaged. In the example, the next boxcar in the example above would be from points 36-45). Moving averaging was applied after the fact to the computed isotope ratio results for the individual scan measurements acquired by the mass spectrometer.

Results and Discussion

Continuous infusion of "bulk" solutions - Three consecutive acquisitions of 100 scans each were collected sequentially, as per the previous uranium isotope ratio measurements.[20, 29] Moving averaging of different scan window sizes (10 – 100 scans) was applied to the isotope ratios of individual scan measurements for all 300 scans collected. As with the previous work, the average across all 300 scans was also

computed. The total analysis time for 300 scans was 13.7 minutes. The isotope ratios for each individual scan, the different scan window sizes, and the 300-scan average are presented in Fig. 3. Results for moving average scan window sizes of 10-100 scans are shown in Fig. 3. As seen, there is a dramatic improvement in the precision of the measurements at even modest scan window sizes.

It must be noted that there is a negative determinate error in the determined values versus the MC-ICP-MS determined value of 0.007277 for this sample, presented as the solid red line in the figure. The tendency for lower $^{235}U/^{238}U$ values on this platform has been addressed in prior publications, being a product of the instrument's data processing protocol as well as basic particle physics within the orbitrap cell.[16, 20, 40] The accuracy of the determined values is a different topic and is outside the scope of this manuscript which is focused on improvements in precision. Of note, the values reported herein are reported without the use of any mass bias correction, which is a common practice in isotope ratio determinations that corrects for biases inherent in the measurement process.[7, 13, 41]

As a practical matter, it was hoped that the use of the moving average method would reduce the analysis time, and thus sample consumption, necessary to achieve consistent isotope ratio (IR) values. The reduction in analysis time afforded by the method is illustrated in Fig 4 for the case of the first 100 data points of the standard 300-scan data acquisition. Figure 4a shows the difference in %RSD values obtained between the continuous (no averaging) case and when averaging windows of 10 and 20 scans are employed. As shown, the %RSD is far better for the moving average case, with the larger scan window providing better precision, as anticipated. What is clear as

well is that successive accumulation of the per scan data does not reduce the overall %RSD as might be initially thought. In fact, the more correct way to view improvements in measurement precision is in the context of the standard error of the mean as successive scans are processed. The standard error of the mean is a measure of how the sample mean varies around the population mean, the true value for sample measurements.[42] Figure 4b shows the corresponding standard error of the mean after at least 10 data points have been included in the standard deviation and illustrates how the quantities change with analysis time using the continuous and moving average data. In this light, the anticipated improvements as a function of the number of samplings (time) are clear. In this vein, the anticipated standard error in the mean decreases by ~ $n^{1/2}$ as shown in the fit response curve and the regression equation. Seen as well is the clear benefit of the moving average data treatment, as the standard errors are far less than in the individual scan data. Most importantly, it is seen that the analysis time to provide high stable IR values is less than 90 seconds in the case of the 20-point boxcar width, whereas the continuous data has still not reached a stable situation after 275 seconds. Thus the anticipated benefits are realized here.

To illustrate and better understand the improvements in the precision of the isotope ratios with increasing scan window sizes, the %RSD of the isotope ratios are plotted vs. the size of the moving average window size and shown in Fig. 5. It should be pointed out that the first data point represents the precision across the 300 individual scans. Clearly seen, the precision improves as the number of points included in the data window is increased. In fact, as shown in the fit, the improvement is just as expected for Poisson statistics, with an $n^{1/2}$ dependence. In many respects, this level of

agreement validates the efficacy of the moving average approach towards uranium isotope ratio precision. As final evidence of the utility of the moving average approach, Fig. 6 presents the cumulative accuracy and precision as a function of the number of scans included in the window. In this box and whisker plot, solid boxes represent the range of points between the end of the 1st quartile and the end of the 3rd quartile (50% of data points), while the whiskers represent the start of the 1st quartile and the end of the 4th quartile. As can be seen, while the precision is certainly improved, the centroid of the values remains consistent, though perhaps increasing some via better S/N characteristics. The dotted line across the figure represents the average value of the isotope ratios across all of the scan window sizes. In general, the average values tend to increase (though not to a statistically significant extent) with the number of scans included in the scan window, which is believed to be due to a reduction in the influences of low points (the fourth quartile consistently has the largest spread) on the overall average with increasing scan window size. Based on these significant improvements in precision, it is rationalized that by applying the moving average method to isotope ratio measurements, the number of total scans needed to produce target-level results could be reduced, thus reducing analysis times and/or sample volumes as demonstrated in Fig 4.

Discrete injections of volume-limited solutions - There is a consistent challenge in the field of isotope ratio mass spectrometry in terms of how much sample must be analyzed to achieve the target levels of precision and accuracy. This is particularly true for samples of nuclear forensics interest, where raw volumes are either very small and/or operator exposure must be minimized. Thus, there is a need to characterize the ability

to capture sufficient data and achieve sufficient statistical performance on signals which are likely transient (i.e., not constant in time) in nature. By extension, this situation is relevant for samples introduced in the course of chromatographic separations, as is common in many IR applications. Ideally, there is some amount of time in which the signals of the respective species reach a steady state for sufficiently long times to allow for adequate sampling. Almost by definition, the analysis of volume-limited samples occurs under non-steady-state signal conditions. Herein lies the benefit of detection schemes wherein all relevant signals are monitored simultaneously, as in the case of multi-collector, time-of-flight, and indeed Fourier transform mass spectrometers such as the Orbitrap. That said, such measurements are still challenging. As an example, Vanhaecke and co-workers have recently described very detailed studies of the roles of detection dwell times and mass window widths in the coupling of high-performance ion chromatography (HPIC) with MC-ICP-MS.[43]

Based on the performance presented above, it was believed that the use of the moving average might allow for better utilization of transient data. To this end, additional studies were conducted on 100 µL injections of 100 ng mL^{-1} natural uranium solutions as a means of reducing both the sample volume and extracting higher IR precision from signals which are transient in nature. Typically, injection measurements are made using just the transient maximum for determinations. As depicted in Fig. 7 for the total ion current chromatogram for a typical 100 µL injection on the LS-APGD/Orbitrap system, the output of the ionization source does not reach a true steady-state (plateau) across the injection volume. According to the total ion response profile in the figure, a seven-minute acquisition (154 scans) was performed on the 100

μL injection. For the moving average analysis, the isotope ratios found for the transient's front and tail were processed, beginning with scan 34 and ending at scan 131, making better utilization of the sample's complete response.

The effects of applying different scan window sizes to the isotope ratios found and the individual scan isotope ratio determinations are shown in Fig. 8. As in the case of the direct infusion responses, the temporal variability is very much buffered with the increasing size of the window; this is particularly true for the data obtained on the ascending and descending portions of the transient. As the total number of scans was only 98, this practically limited the size of the windows to no more than 50 scans. As might be expected, the variation in the raw values is greatly lessened in the central portion of the transient (identified as the plateau in Fig. 7), as would be expected. And while the variability improves in this region, the absolute IR values are increased, suggesting better recoveries of the minor ^{235}U signals. This agrees with the data presented in Fig. 6 for the continuous infusion case.

To highlight the specific level of improvement realized with the moving average approach, Fig. 9 presents the total ion transient, along with the single scan $^{235}U/^{238}U$ isotope ratio values and the moving average values for the case of the 25-scan window. Again, far greater variability in the single-scan IR values is seen on the leading and trailing edges of the transient, with the horizontal bars added to guide the eye representing $\pm$ 5% deviations of the average found for the single-scan values. This variability is improved overall using the moving average (green line), but in addition, the moving average allows for the data in the leading and trailing edges to be used in the data set. As a point of reference, using the central ~50% centroid of the transient

(nominally scans 65-95), as suggested by Vanhaecke et al.,[43] yields a $^{235}U/^{238}U$ precision of 3.3 %RSD for the single-point data, while the 25-point window applied across those data points yields a value of 0.2 %RSD across that same window. As such, the moving average adds great improvements in precision, even for the most-consistent portions of the transient response.

The respective improvements in the cross-transient isotope ratio precision as a function of boxcar size are depicted in Fig. 10. The first point of comparison with the direct infusion case (Fig. 6) is the fact that the single scan precision across the transient (~5.2 %RSD) is degraded relative to the steady operation (~3.4 %RSD), as expected. As in the case of the continuous infusion analysis, increasing the number of scans encompassing the window has a profound effect, again yielding the expected $n^{1/2}$ proportionality. In fact, for the 50 scan window, the 0.54 %RSD precision derived for the transient data is very similar to the 0.44 %RSD seen for the continuous infusion case. The key here is that the data for the continuous infusion was acquired over a time span of 13.7 min for 300 total scans, while that for the transient represents only 4.4 min of analysis time and a total of 98 scans. Taken a step further, the 50-scan window in the transient case only employs the central 49 scans, as the window rolls across the total scan count, whereas in the continuous case, there are a total of 251, 50-scan data points comprising the data set.

Conclusions

The preliminary findings of the use of moving average analysis for isotopic ratio determinations for the LS-APGD coupled with an Orbitrap mass spectrometer present substantial improvements in precision over the cumulative averaging of scans across an

entire acquisition. The benefits of the moving average approach were very straightforward for the case of continuous infusion of test solutions, with the expected $n^{1/2}$ improvement in precision realized for the use of windows of increasing scan numbers. In fact, this relationship reveals that even at a challenging $^{235}U/^{238}U$ of ~0.0073, the system still follows Poisson statistics. It was clearly demonstrated that the relevant consideration of the standard error of the mean of the accumulated data reveals that dramatic reductions in analysis time and sample volumes can be achieved, while still providing more precise IR values. The ability to characterize and predict levels of measurement precision will allow for better logistical planning of measurements tailored to meet target levels of precision without wasting time and resources. In fact, the goal here was not to obtain ultimate levels of precision but to point to rational means of improving the overall process. In addition, this study is not focused on the accuracy of the isotope ratio found, only on the reduction of the temporal variation in the measurement. Future studies will focus on accuracy with mass bias corrections applied.

These findings have led to the use of moving averaging as a means of achieving improved performance for discrete sample injections rather than direct infusion techniques for sample introduction to the LS-APGD ionization source. The use of the moving average method allows for more effective use of samples while analytical responses are temporally evolving, i.e., performing measurements outside of steady-state conditions. Here again, Poisson statistics are obeyed, even for temporally varying signals. This is a key attribute of the present studies as it points again to a means of tailoring experiments to yield the targeted levels of isotope ratio measurement precision

in those cases where sample volumes are limited or time is of the essence. Ultimately, these efforts contribute to the fundamental literature supporting the use of Orbitrap mass spectrometry, particularly in the case of sampling the LS-APGD, in the area of high-resolution isotope ratio mass spectrometry.

Acknowledgments

This work was supported by the Oak Ridge National Laboratory, managed by UT-Battelle for the Department of Energy under Contract DE-AC05-000R22725. This work was funded by the United States National Nuclear Security Administration's Office of Defense Nuclear Nonproliferation Research & Development

Conflicts of interest

The authors declare no competing financial interests.

References

1. Ireland, T. R., Recent developments in isotope-ratio mass spectrometry for geochemistry and cosmochemistry. *Rev. Sci. Instrum.* **2013,** *84* (1), 011101.

2. Benson, S.; Lennard, C.; Maynard, P.; Roux, C., Forensic applications of isotope ratio mass spectrometry—A review. *Forensic Sci. Int.* **2006,** *157* (1), 1-22.

3. Gentile, N.; Siegwolf, R. T. W.; Esseiva, P.; Doyle, S.; Zollinger, K.; Delémont, O., Isotope ratio mass spectrometry as a tool for source inference in forensic science: A critical review. *Forensic Sci. Int.* **2015,** *251*, 139-158.

4. Mayer, K.; Wallenius, M.; Ray, I., Nuclear forensics—a methodology providing clues on the origin of illicitly trafficked nuclear materials. *Analyst* **2005,** *130* (4), 433-441.

5. Kristo, M. J.; Tumey, S. J., The state of nuclear forensics. *Nucl. Instrum. Methods B* **2013,** *294*, 656-661.

6. *Identification of High Confidence Nuclear Forensics Signatures*. INTERNATIONAL ATOMIC ENERGY AGENCY: Vienna, 2017.

7. Boulyga, S.; Konegger-Kappel, S.; Richter, S.; Sangély, L., Mass spectrometric analysis for nuclear safeguards. *J. Anal. At. Spectrom.* **2015,** *30* (7), 1469-1489.

8. Eppich, G. R.; Mácsik, Z.; Katona, R.; Konegger-Kappel, S.; Stadelmann, G.; Köpf, A.; Varga, B.; Boulyga, S., Plutonium assay and isotopic composition measurements in nuclear safeguards samples by inductively coupled plasma mass spectrometry. *J. Anal. At. Spectrom.* **2019,** *34* (6), 1154-1165.

9. Richter, S.; Kühn, H.; Aregbe, Y.; Hedberg, M.; Horta-Domenech, J.; Mayer, K.; Zuleger, E.; Bürger, S.; Boulyga, S.; Köpf, A.; Poths, J.; Mathew, K., Improvements in routine uranium isotope ratio measurements using the modified total evaporation method for multi-collector thermal ionization mass spectrometry. *J. Anal. At. Spectrom.* **2011,** *26* (3), 550-564.

10. Marin, R. C.; Sarkis, J. E. S.; Nascimento, M. R. L., The use of LA-SF-ICP-MS for nuclear forensics purposes: uranium isotope ratio analysis. *J. Radioanal. Nucl. Chem.* **2013,** *295* (1), 99-104.

11. Aggarwal, S. K., Thermal ionisation mass spectrometry (TIMS) in nuclear science and technology – a review. *Anal. Methods* **2016,** *8* (5), 942-957.

12. Martelat, B.; Isnard, H.; Vio, L.; Dupuis, E.; Cornet, T.; Nonell, A.; Chartier, F., Precise U and Pu Isotope Ratio Measurements in Nuclear Samples by Hyphenating Capillary Electrophoresis and MC-ICPMS. *Anal. Chem.* **2018,** *90* (14), 8622-8628.

13. Yang, L., Accurate and precise determination of isotopic ratios by MC-ICP-MS: A review. *Mass Spectrom. Rev.* **2009,** *28* (6), 990-1011.

14. Weiedmeyer, T. W. M. a. R. H., A Table of Polyatomic Interferences in ICP-MS. *At. Spectrosc.* **1998,** *19*, 150-155.

15. Metzger, S. C.; Manard, B. T.; Bostick, D. A.; Ticknor, B. W.; Rogers, K. T.; McBay, E. H.; Glasgow, D. C.; Zirakparvar, N. A.; Hexel, C. R., An approach to separating Pu, U, and Ti from high-purity graphite for isotopic analysis by MC-ICP-MS. *J. Anal. At. Spectrom.* **2021,** *36* (6), 1150-1158.

16. Bills, J. R.; Nagornov, K. O.; Kozhinov, A. N.; Williams, T. J.; Tsybin, Y. O.; Marcus, R. K., Improved Uranium Isotope Ratio Analysis in Liquid Sampling–Atmospheric Pressure Glow Discharge/Orbitrap FTMS Coupling through the Use of an External Data Acquisition System. *J. Am. Soc. Mass Spectrom.* **2021,** *32* (5), 1224-1236.

17. Hoegg, E. D.; Barinaga, C. J.; Hager, G. J.; Hart, G. L.; Koppenaal, D. W.; Marcus, R. K., Isotope ratio characteristics and sensitivity for uranium determinations using a liquid sampling-atmospheric pressure glow discharge ion source coupled to an Orbitrap mass analyzer. *Journal of Analytical Atomic Spectrometry* **2016,** *31* (12), 2355-2362.

18. Perkins, A. A.; Hoegg, E. D.; Marcus, R. K., Evaluation of the powering modes and geometries of the Liquid Sampling – Atmospheric Pressure Glow Discharge – Orbitrap system for analytical performance and isotope ratio analysis. *Spectrochim. Acta B - At. Spectrosc.* **2021,** *176*, 106044.

19. Paing, H. W.; Manard, B. T.; Ticknor, B. W.; Bills, J. R.; Hall, K. A.; Bostick, D. A.; Cable-Dunlap, P.; Marcus, R. K., Rapid Determination of Uranium Isotopic Abundance from Cotton Swipes: Direct Extraction via a Planar Surface Reader and Coupling to a Microplasma Ionization Source. *Anal. Chem.* **2020,** *92* (12), 8591-8598.

20. Hoegg, E. D.; Manard, B. T.; Wylie, E. M.; Mathew, K. J.; Ottenfeld, C. F.; Marcus, R. K., Initial Benchmarking of the Liquid Sampling-Atmospheric Pressure Glow Discharge-Orbitrap System Against Traditional Atomic Mass Spectrometry Techniques for Nuclear Applications. *J. Am. Soc. Mass Spectrom.* **2019,** *30* (2), 278-288.

21. Marcus, R. K.; Manard, B. T.; Quarles, C. D., Liquid sampling-atmospheric pressure glow discharge (LS-APGD) microplasmas for diverse spectrochemical analysis applications. *J. Anal. At. Spectrom.* **2017,** *32* (4), 704-716.

22. Zhang, L. X.; Marcus, R. K., Mass spectra of diverse organic species utilizing the liquid sampling-atmospheric pressure glow discharge (LS-APGD) microplasma ionization source. *J. Anal. At. Spectrom.* **2016,** *31* (1), 145-151.

23. Williams, T. J.; Marcus, R. K., Coupling the liquid sampling – atmospheric pressure glow discharge, a combined atomic and molecular (CAM) ionization source, to a reduced-format mass spectrometer for the analysis of diverse species. *J. Anal. At. Spectrom.* **2020,** *35* (9), 1910-1921.

24. Hoegg, E. D.; Williams, T. J.; Bills, J. R.; Marcus, R. K.; Koppenaal, D. W., A multi-electrode glow discharge ionization source for atomic and molecular mass spectrometry. *J. Anal. At. Spectrom.* **2020,** *35* (9), 1969-1978.

25. Williams, T. J.; Bills, J. R.; Marcus, R. K., Mass spectrometric characteristics and preliminary figures of merit for polyaromatic hydrocarbons via the liquid sampling-atmospheric pressure glow discharge microplasma. *J. Anal. At. Spectrom.* **2020,** *35* (11), 2475-2478.

26. Hoegg, E. D.; Godin, S.; Szpunar, J.; Lobinski, R.; Koppenaal, D. W.; Marcus, R. K., Ultra-High Resolution Elemental/Isotopic Mass Spectrometry ($m/\Delta m > 1{,}000{,}000$): Coupling of the Liquid Sampling-Atmospheric Pressure Glow Discharge with an Orbitrap Mass Spectrometer for Applications in Biological Chemistry and Environmental Analysis. *J. Am. Society Mass Spectrom.* **2019,** *30* (7), 1163-1168.

27. Paing, H. W.; Bryant, T. J.; Quarles, C. D.; Marcus, R. K., Coupling of Laser Ablation and the Liquid Sampling-Atmospheric Pressure Glow Discharge Plasma for Simultaneous, Comprehensive Mapping: Elemental, Molecular, and Spatial Analysis. *Anal. Chem.* **2020,** *92* (18), 12622-12629.

28. Marcus, R. K.; Hoegg, E. D.; Hall, K. A.; Williams, T. J.; Koppenaal, D. W., Combined Atomic and Molecular (CAM) Ionization with the Liquid Sampling-Atmospheric Pressure Glow Discharge Microplasma. *Mass Spectrom. Rev.* **2021,** *in press*.

29. Hoegg, E. D.; Marcus, R. K.; Hager, G. J.; Hart, G. L.; Koppenaal, D. W., Concomitant ion effects on isotope ratio measurements with liquid sampling – atmospheric pressure glow discharge ion source Orbitrap mass spectrometry. *J. Anal. Atom. Spectrom.* **2018,** *33* (2), 251-259.

30. Lange, O.; Damoc, E.; Wieghaus, A.; Makarov, A., Enhanced Fourier transform for Orbitrap mass spectrometry. *International Journal of Mass Spectrometry* **2014,** *369*, 16-22.

31. Xian, F.; Corilo, Y. E.; Hendrickson, C. L.; Marshall, A. G., Baseline correction of absorption-mode Fourier transform ion cyclotron resonance mass spectra. *Int. J. Mass Spectrom.* **2012,** *325-327*, 67-72.

32. Yang, L.; Sturgeon, R. E., Comparison of mass bias correction models for the examination of isotopic composition of mercury using sector field ICP-MS. *Journal of Analytical Atomic Spectrometry* **2003,** *18* (12), 1452-1457.

33. Mathew, K. J.; O'Connor, G.; Hasozbek, A.; Kraiem, M., Total evaporation method for uranium isotope-amount ratio measurements. *Journal of Analytical Atomic Spectrometry* **2013,** *28* (6), 866-876.

34. Williams, T. J.; Hoegg, E. D.; Bills, J. R.; Marcus, R. K., Roles of collisional dissociation modalities on spectral composition and isotope ratio measurement

performance of the liquid sampling – atmospheric pressure glow discharge / orbitrap mass spectrometer coupling. *Int. J. Mass Spectrom.* **2021,** *464*, 116572.

35. Azami, H.; Mohammadi, K.; Bozorgtabar, B., An Improved Signal Segmentation Using Moving Average and Savitzky-Golay Filter. *J. Signal Inform. Process.* **2012,** *3*, 39-44.

36. Amneh, A. A.-M., Application of Moving Average Filter for the Quantitative Analysis of the NIR Spectra. *J. Anal. Chem.* **2019,** *74* (7), 686-692.

37. Savitzky, A.; Golay, M. J. E., Smoothing and differentiation of data by simplified least squares procedures. *Analytical Chemistry* **1964,** *36*, 1627.

38. Press, W. H.; Teukolsky, S. A., Savitzky-Golay Smoothing Filters. *Computers in Physics* **1990,** *4* (6), 669-672.

39. Gorry, P. A., General least-Squares smoothing and differentiation by the convolution (Savitsky-Golay) method. *Anal. Chem.* **1990,** *62*, 570-573.

40. Hofmann, A. E.; Chimiak, L.; Dallas, B.; Griep-Raming, J.; Juchelka, D.; Makarov, A.; Schwieters, J.; Eiler, J. M., Using Orbitrap mass spectrometry to assess the isotopic compositions of individual compounds in mixtures. *Int. J. Mass Spectrom.* **2020,** *457*.

41. Heumann, K. G.; Gallus, S. M.; Radlinger, G.; Vogl, J., Precision and accuracy in isotope ratio measurements by plasma source mass spectrometry. *J. Anal. At. Spectrom.* **1998,** *13* (9), 1001-1008.

42. Miller, J. N., Miller, J.C., *Statistics and Chemometrics for Analytical Chemistry*. 4th ed.; Pearson Education Limited: Drochester, United Kingdom, 2000; p 271.

43. Wanna, N. N.; Van Hoecke, K.; Dobney, A.; Vasile, M.; Cardinaels, T.; Vanhaecke, F., Determination of the lanthanides, uranium and plutonium by means of on-line high-pressure ion chromatography coupled with sector field inductively coupled plasma-mass spectrometry to characterize nuclear samples. *J. Chromatogr. A* **2020,** *1617*, 460839.

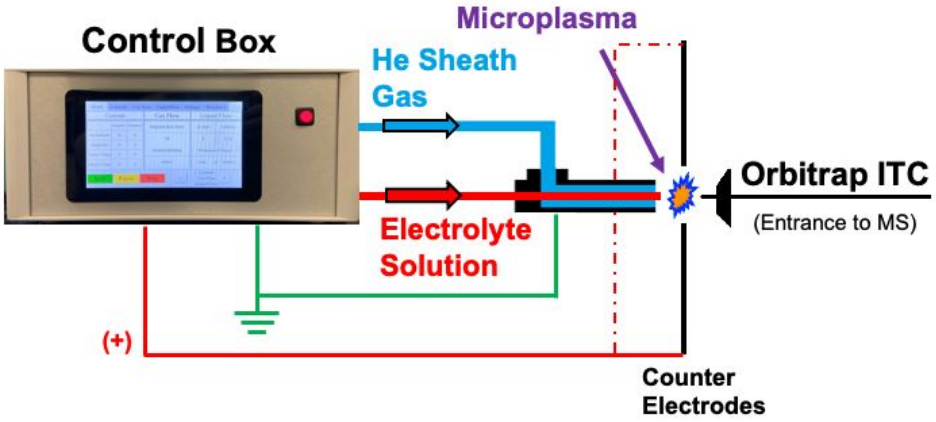

Fig. 1

Figure 1. Graphic depiction of the components of the dual electrode, liquid sampling-atmospheric pressure glow discharge (LS-APGD) ionization source, and controller unit.

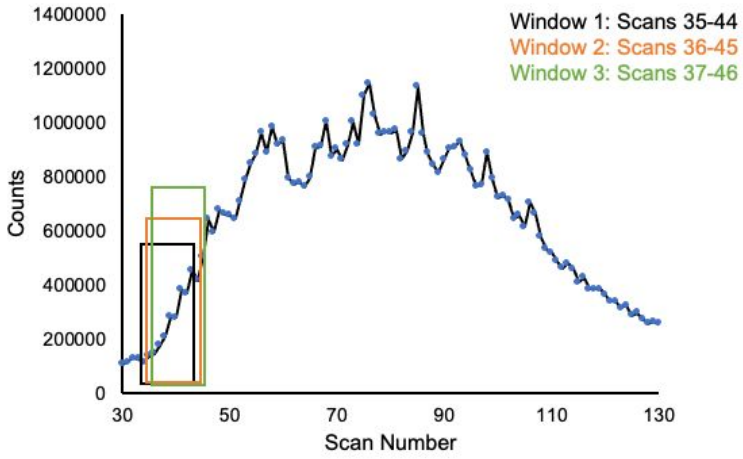

Fig. 2

Figure 2. Graphic illustration of the concept of the moving average methodology for a generic transient signal.

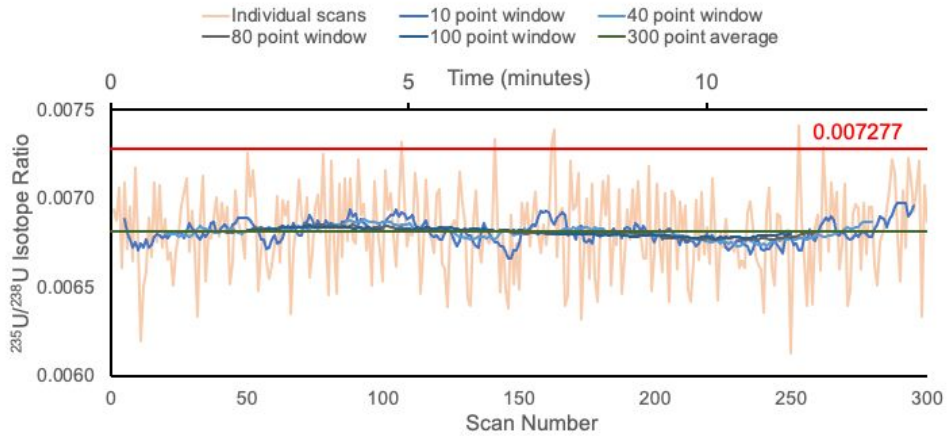

Fig. 3

Figure 3. Individual scan and moving average $^{235}U/^{238}U$ values as a function of window width. The solid horizontal line represents MC-ICP-MS determined $^{235}U/^{238}U$ value for the test solution.

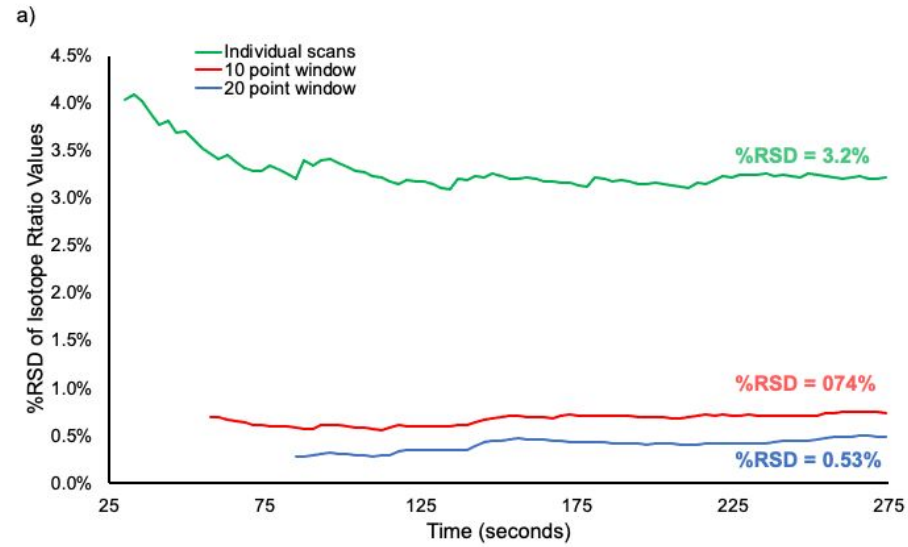

Fig. 4a

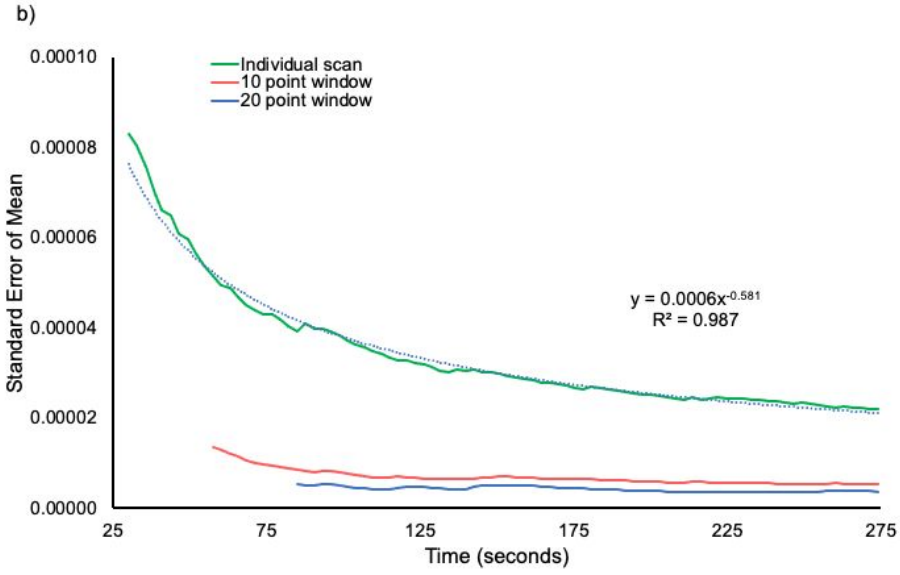

Fig. 4b

Figure 4. Comparison of $^{235}U/^{238}U$ precision as a function of scan number for continuous (no averaging) processing and the use of moving average with 10- and 20-point window widths. a) Data presented in regards to the cumulative %RSD as a function of the number of scans. b) Data presented in regards to the standard error of the mean as a function of the number of scans. The start of each line is at the point where at least 10 data points are included in the standard deviation calculation.

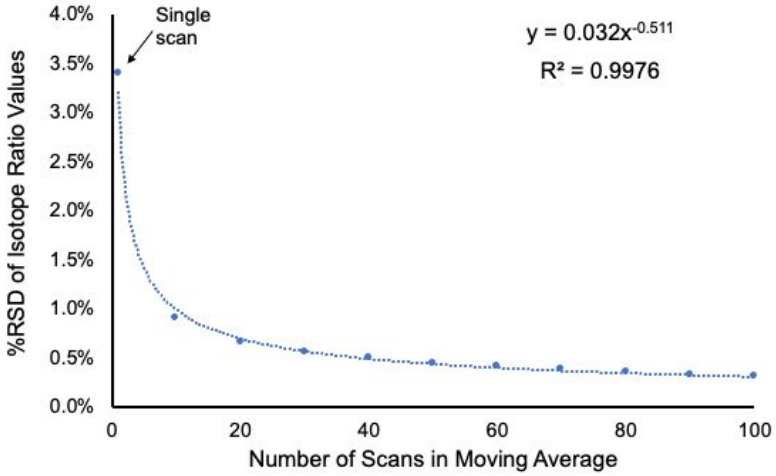

Fig. 5

Figure 5. Precision of determined $^{235}U/^{238}U$ values as a function of averaging window width.

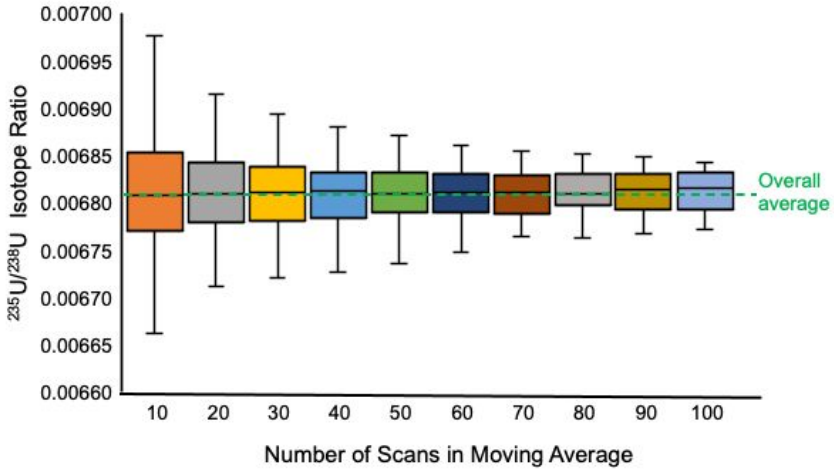

Fig. 6

Figure 6. Graphic depiction of the effects of averaging window width on isotope ratio precision and accuracy.

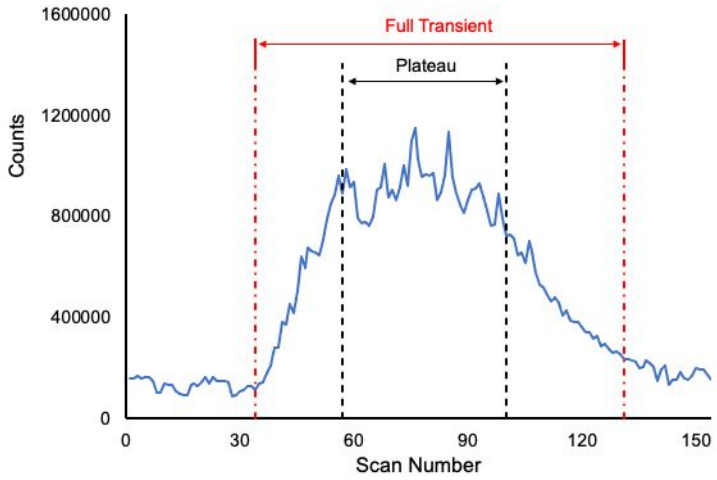

Fig. 7

Figure 7. Graphic depiction of the typical “plateau” data acquisition region along with a signal transient (such as a liquid injection) along with the complete transient coverage afforded by the use of the moving average data processing procedure. The graphic represents the total ion chromatogram from 263.5 - 273.5 Da (encompassing all U isotope responses) as a function of scan number.

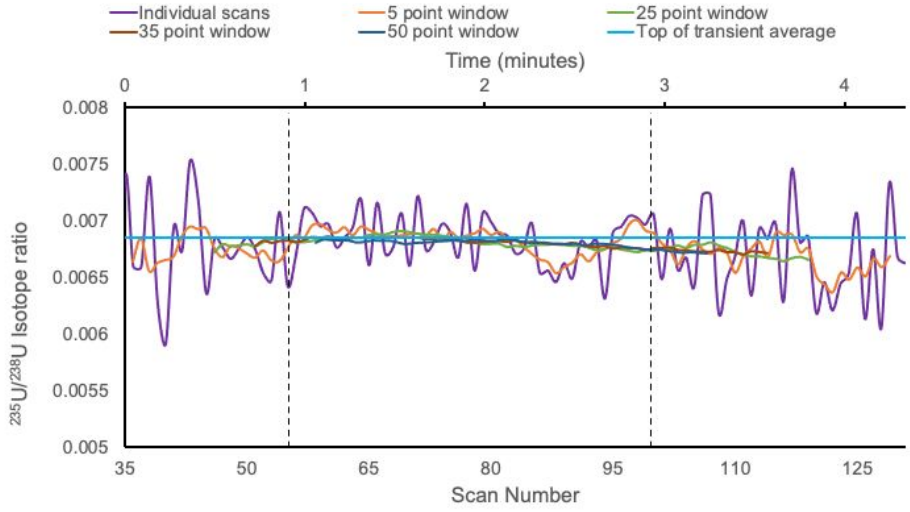

Fig. 8

Figure 8. Individual scan and moving average $^{235}U/^{238}U$ values as a function of averaging window width across the 100 μL injection transient.

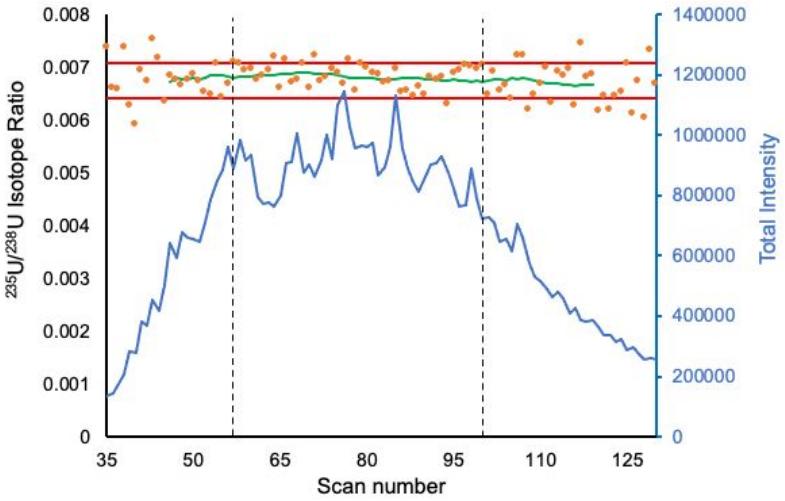

Fig. 9

Figure 9. Scatter plot of the individual scan $^{235}U/^{238}U$ values as well as the trace realized in the use of the 25-scan moving average (red bars represent ±5 % of the average of all scans).

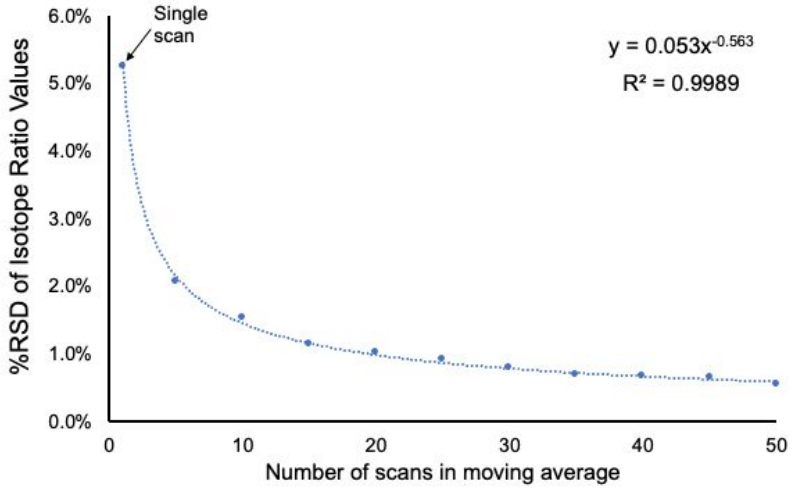

Fig. 10

Figure 10. Precision of determined $^{235}U/^{238}U$ values as a function of window width for the 100 μL injection transient.